https://doi.org/10.20965/ijat.2017.p0907

Paper:

Effects of Adhesives on Reliability in Interfacial Strength Evaluation Method for Plasma-Sprayed Hydroxyapatite Coating

Yuichi Otsuka†, Yoshihisa Hiraki, Yuki Hakozaki, Yukio Miyashita, and Yoshiharu Mutoh

Nagaoka University of Technology
1603-1 Kamitomioka, Nagaoka, Niigata 940-2188, Japan
†Corresponding author, E-mail: otsuka@vos.nagaokaut.ac.jp
[Received February 9, 2017; accepted May 29, 2017]

The purpose of this study is to evaluate interfacial strength of plasma-sprayed HAp coating by using more general adhesives. Plasma-sprayed HAp coating has been applied to bond bones with the surfaces of artificial hip joints. However, HAp coating is subjected to crack or delamination by mechanical loading. Conventional standard codes for measurement of interfacial strength of calcium phosphate coating determine the use of a specific adhesive irrationally. Our group previously proposed pre-immersion treatment process in preparation of interfacial testing specimens in order to obtain valid value of interfacial strength. However, the type of the adhesive was for medical purpose and not general one. To widen applicability of the proposed method, a selection policy of adhesive is indispensable. Metal Lock Y610 (ML adhesive) was selected as one of general adhesives. Interfacial strength tests by using ML adhesive were conducted. The results of interfacial strength test were compatible with the one reported by previous study, which suggest that the selection of general type of adhesive was successful. Raman spectroscopy analyses were also conducted to confirm a suppressed infiltration of ML adhesives.

Keywords: hydroxyapatite, plasma-sprayed coating, interfacial strength, adhesives

1. Introduction

Hydoxyapatite (HAp) coating has been widely used for metallic components in biomedical field [1, 2]. In order to improve performance of HAp coating, various technologies such as composites, surface treatments, complexation, etc., have been successfully applied [3–8]. However, HAp coating has a risk of failure by loading in use [9]. There has been many researches for failure behavior of HAp coating, such as bending failure, dissolution behavior, corrosion fatigue failure by cyclic loading [10–15]. In regulation process on medical devise, tensile interfacial strength of HAp coating must be determined. ISO standard and ASTM standard determine brief processes on measurement of interfacial strength of HAp coating [16, 17]. On the other hand, Scherrer et al. reviewed scatters in the result of "interfacial strength" of HAp coating by various loading methods and challenged the reported results that considerable large scatterer existed due to lacks on determination of failure modes, loading method and effects of adhesive [18]. Hakozaki et al. pointed out that infiltration effects of adhesive was critical in determination process of interfacial strength [19]. They proposed a prevention method to infiltration of adhesives during attachment procedure of specimens. Their results demonstrated the same average regardless of specimen diameters and small ratio of infiltration of adhesives, which can be regarded as valid interfacial strength. Though their proposed method was effective in reducing scattering effects of an adhesive, the adhesive they used is still limited. In order to widen applicability of the reliable interfacial strength testing method, a selection policy of adhesives must be considered.

This study aims at proposing the selection policy of adhesives in interfacial strength testing by comparing the results used by different adhesives. Metal Lock Y610 (Cemedine) was selected as an example of general adhesives because of its similar physical and mechanical properties as shown in **Table 1**. Effects of diameters or types of adhesives on values of interfacial strength of HAp coating were subsequently observed. Infiltration ratio of the adhesive was observed by using image processing or Raman spectroscopy. Finite element analyses was also conducted in order to discuss locations or amount of infiltrations on scattering effects of testing results. Finally, a selection policy of adhesives was discussed.

2. Experimental Procedures

The specimen were made of Ti6Al4V-ELI. The specimens were machined in a cylinder shape with diameter 15 and 25 mm with length of 60 mm, as shown in **Fig. 1**. HAp powder (HAP-100 TAIHEI CHEMICAL INDUSTRIAL Co., Ltd.) with powder size less than 90 μm was deposited by atmospheric plasma spraying. Before the plasma spray process, cross sectional surfaces were

Table 1. Physical and mechanical properties of adhesives.

Adhesive type	Physical property			Mechanical property	
	Operative time [min]	Hardening time [min]	Hardening type	Young's modulus [GPa]	Adhesive strength [MPa]
Superbond (medical use)	2	8	Ambient temperature	1.9	38
Metal Lock Y610 (general use)	3	60	Ambient temperature	0.7	22

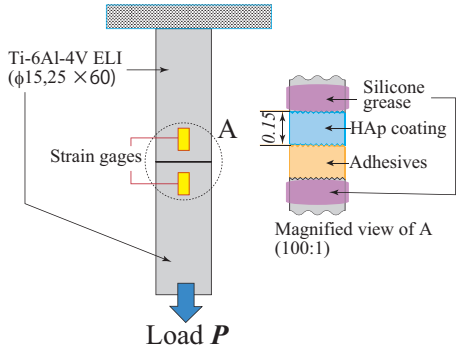

Fig. 1. Configuration of interfacial strength test specimen [19].

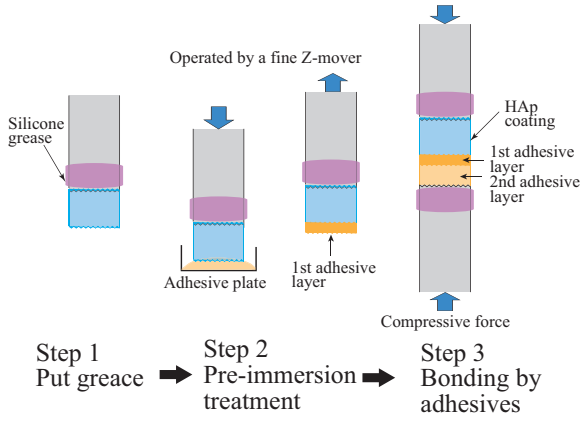

Fig. 2. Bonding process of interfacial strength test specimens proposed by Hakozaki et al. [19].

treated by grid blasting using alumina particle #30, spraying pressure of 5 MPa. Plasma spray conditions were 68 V, current 500 A, spraying distance 120 mm, particle supply 20 g/min, flow rate 120 mm/s, target thickness of 100–150 μm, respectively. During the plasma spraying process, all specimens are randomly selected up and fixed by heat-resistant tapes in order to reduce biases in coating properties between both diameter series.

Figure 2 shows an adhesion process of interfacial test specimens proposed by Hakozaki et al. [19]. A grease was uniformly put onto the side surface of every specimen before the adhesion in order to prevent excessive attachment of the adhesives on the side surface.

Interfacial test following the method of ISO13779-4:2002 was conducted by the autograph AGS-X 10N-10kN (Shimadzu Co., Ltd.) with a cross head displacement rate of 1 mm/min. Strain gages were attached on the points of 10 mm from coating layer in order to record strain in the substrate during the interfacial strength tests. Values of interfacial strength were calculated by maximum load divided by nominal area.

Digital microscope (VHX-1000, Keyence) was used to detect remaining coating or adhesives on the fracture surface of interfacial specimens. Pictures were binarized and infiltration ratio was defined by the value of adhesive area divided by nominal area of fracture surface. Raman spectroscopy (Lab-RAM HR-800, Horiba Jobin YVON) was also used in order to detect infiltrations of adhesives into HAp coating. The measurement conditions were as the follows; laser wavelength of 532 nm, laser power of 50 mW, objective lenz ×50, observation area 500×500 μm, increments of each measurement for X and Y directions of 10 μm, respectively. Each material was identified by the strongest peak range in each spectra; TiO_2; 420–450 cm^{-1}, HAp; 920–950 cm^{-1}, Metal Lock Y610; 1420–1480 cm^{-1}, respectively.

Finite element analyses were conducted to discuss the effect of infiltration types on failure behavior of HAp coating. Marc 2015.0 was used for the calculation. A bond bar with diameter of 15 mm and length of 10 mm was used in modeling. Axysymmetric model was assumed and number of nodes and 4-nodes elements are 9059 and 8400, respectively. A thickness of HAp coating and the one of adhesive layer were set to be 150 μm and they were divided in to 4-node elements whose size are 50×50 μm^2. Young's modulus and poisson's ratio of HAp coating were set to be 70 GPa and 0.24, respectively [14, 15]. Those of titanium alloys were 110 GPa and 0.33. Those of adhesive layer were assumed to be 1.9 GPa and 0.35 by referring to the value of Superbond [20]. Plasticity of any material was not considered in the calculation. Interfacial strength between HAp coating with Ti substrate and the one between adhesive layer with Ti substrate were 38 MPa and 15 MPa, respectively [19]. Young's modulus and poisson's ratio of infiltrated area were calculated by mixed layer of HAp coating and adhesive by the volume ratio of 50%:50%. By changing infiltration area and infiltration ratio from 10% to 50%, the changes in the values of interfacial strength were observed. Though actual failure modes of HAp coating contain both cohesive failure (failure within the layer) and adhesive failure (failure occurred at interfaces) [18], only the adhesive failure (intergfacial failure) was considered in the calculations.

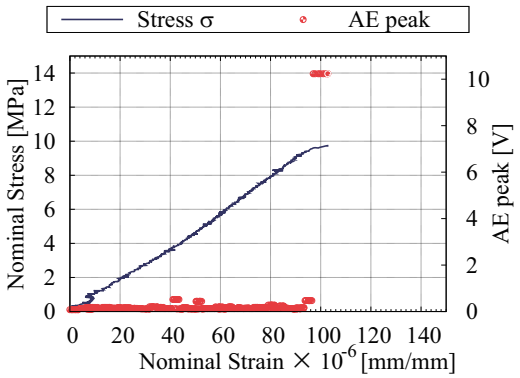

Fig. 3. Stress-strain curves by the specimen bonded by Superbond. Left axis: stress (line curve). Right axis: AE amplitude (closed circle).

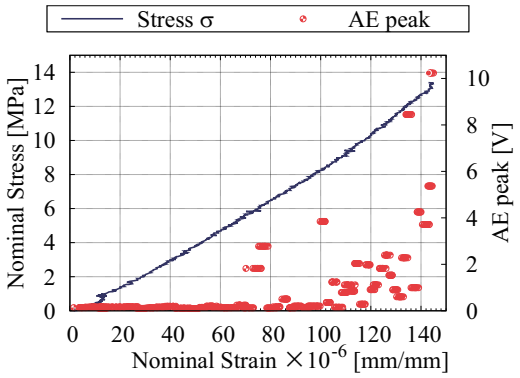

Fig. 4. Stress-strain curves by the specimen bonded by Metal Lock Y610. Left axis: stress (line curve). Right axis: AE amplitude (closed circle).

3. Results and Discussions

Figures 3 and **4** show stress-strain curves of interfacial testing specimen bonded by Superbond [19] and by Metal Lock Y610, respectively. Both the curves have almost same gradient close to Young's modulus of Ti-6Al-4V substrate. The values of gradients of stress-strain curves changed little even after AE signals, which can be the indicator of damages in adhesive layers, had been detected. The result suggests that adhesion conditions can affect little on deformation behavior of specimens though the conditions can vary the value of interfacial strength. On the other hand, acoustic emission (AE) in **Fig. 4** detected some signals at earlier stage before final failure probably due to damages in adhesive layers. Though such the measurement methods are not mandatory in standard codes [16, 17], they are effective in discussing reliability and validity of each testing data, which is a cause of scatters in the results [18].

Figure 5 shows a summary of interfacial strength by two type of adhesives. The figure clearly demonstrates that Metal Lock Y610 (general adhesive) could provide the same result by Superbond (special medical adhesive) with preimmersion treatment. It can be concluded that

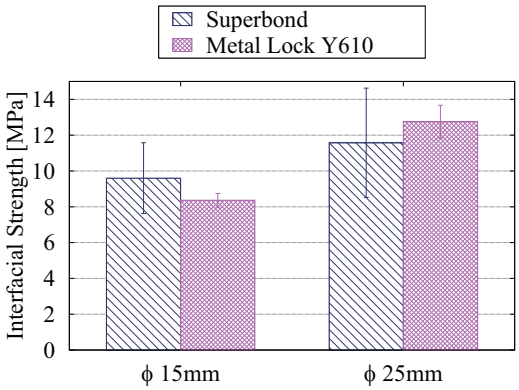

Fig. 5. Comparison of interfacial strength by two adhesives. Data of Superbond was referred by Hakozaki et al. [19]. All samples were applied pre-immersion treatment shown in **Fig. 2**.

the proposed method by Hakozaki et al. [19] can provide reliable values of interfacial strength of HAp coating regardless of adhesive or diameter.

Figure 6 shows an example of fracture surface of HAp coating bonded by Superbond. Though thin layer of HAp coating is remained on the fracture surface, primal failure mode is considered to be adhesive failure that occurred adjacent to the interface between HAp coating with Ti substrate. Adhesive layer at the edge of the fracture surface is observed by higher region in optical image, which is shown by brighter white region in the figure. **Fig. 6(a)** dose not show such the region at the center of specimen and therefore macroscopic infiltration of adhesives in HAp coating did not occur. However, binary image in **Fig. 6(b)** indicated not only remained adhesive layers at the edge but also remained HAp coating on the fracture surfaces. Though infiltration of adhesives is expected, such the limited infiltration is difficult to be detected only by optical images.

Figure 7 shows an example of fracture surface of HAp coating bonded by Metal Lock Y610. Though the edge of adhesive layer was decreased compared with the case in **Fig. 6**, there still exists a thin layer of HAp coating on the fracture surface but the failure mode is unchanged. Those results demonstrated that optical microscope observation is beneficial in determination of failure modes, which has been strongly suggested by the review [18]. However, binary image of **Fig. 7** could not be obtained by using a same threshold value in binarization. HAp coating contain micro pores on the boundary of splats where adhesive can be infiltrated into. Hakozaki et al. [19] reported that it was difficult to distinguish infiltrated adhesive in HAp coating layer only by using image processing. Furthermore, exposure ratio of substrate calculated by binary image showed similar value regardless of prevention of infiltrations. Consequently, another method is necessary to detect the degree of infiltrating adhesives.

Raman spectroscopy was conducted to detect infiltrated adhesives in HAp coating. **Fig. 8** shows a Raman spectra

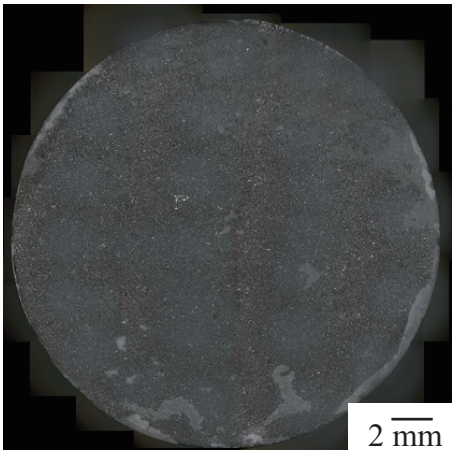

(a) Optical microscope image of fracture surface of HAp coating side of interfacial specimen.

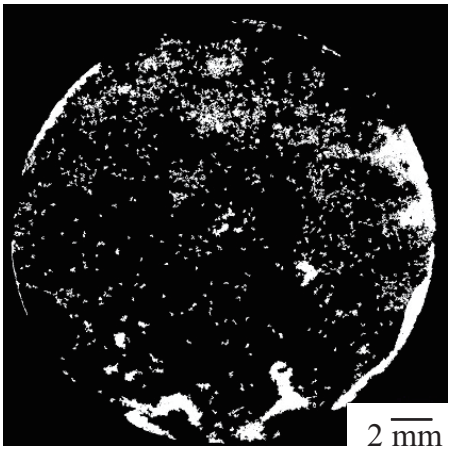

(b) Binary image of the optical microscope image. White area shows adhesive or HAp coating and black area shows exposed Ti substrate, respectively.

Fig. 6. Features of a fracture surface of HAp coating side bonded by Superbond.

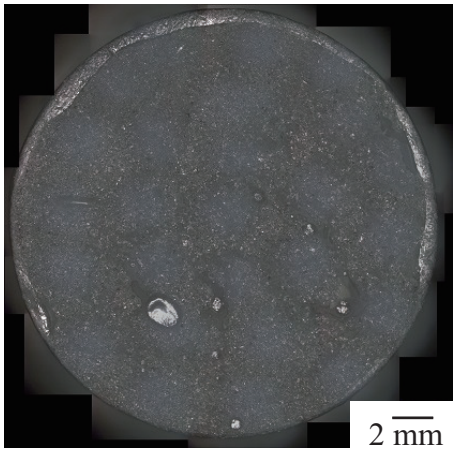

Fig. 7. Features of a fracture surface of HAp coating side bonded by Metal Lock Y610.

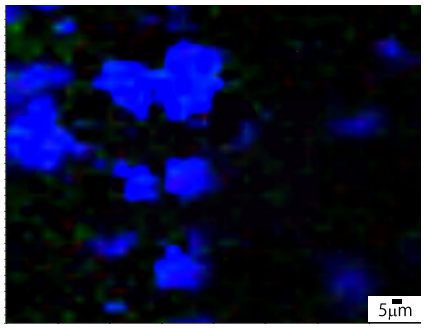

(a) RGB image

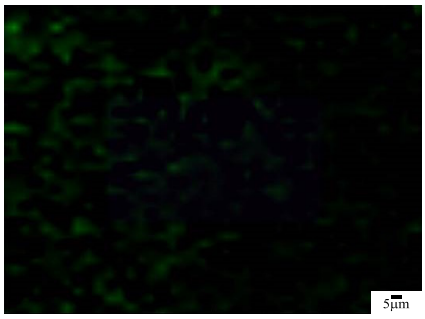

(b) Green image

(c) Binarized image

Fig. 8. Raman spectra mapping on the HAp coating side bonded by Metal Lock Y610. Red area: TiO_2, Blue area; HAp, Green area; Metal Lock Y610, respectively. Black area in (a) and (b) are undetected area of Raman spectra where can be regarded as the surface of metallic Ti-6Al-4V.

mapping on the HAp coating side bonded by Metal Lock Y610. The map successfully identified an infiltrated area of the adhesives. Plasma-sprayed HAp coating normally does not possess inter-connected porosity inside the coating layer [21]. Therefore, the evidence of infiltration of adhesives shown in **Fig. 8** suggested that another paths of infiltration existed such as imperfect contacts between splats in HAp coating layer, which provided micro pores at the interfaces among the splats. Hakozaki et al. [19] also reported the infiltration behavior and degree of infiltration was high at the case of adhesives which has low viscosity. Scherrer et al. suggested that unclear determination on failure position (cohesive/adhesive failure) is problematic factor in reliability of interfacial strength test methods [18]. Our result additionally pointed out the necessity of observing the infiltration ratio of adhesives into coating layers. Infiltrated ratio of the adhesive was then calculated by using binary image of **Fig. 8** which show only an adhesive area. **Fig. 9** shows infiltration ratio of adhesives in the observed region of Raman spectra map-

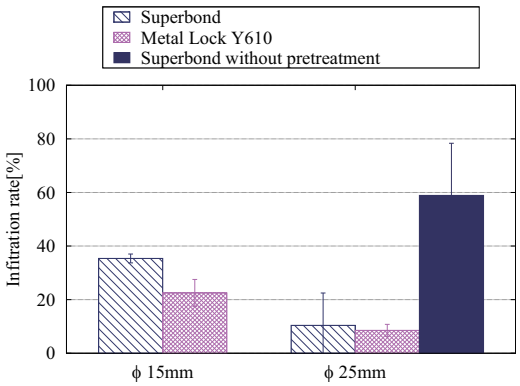

Fig. 9. Infiltration ratios of two adhesives. Data of Superbond was referred by Hakozaki et al. [19].

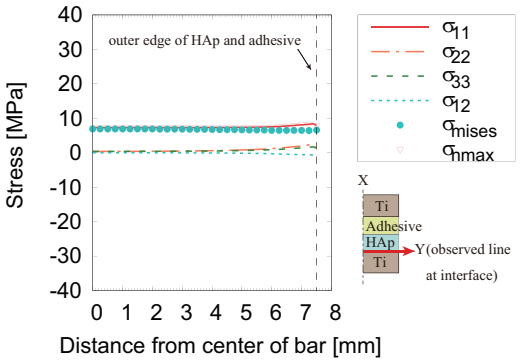

Fig. 10. Stress distribution at the interface between HAp coating and Ti substrate when it was subjected to maximum loading. Infiltration of adhesive into HAp coating was not considered.

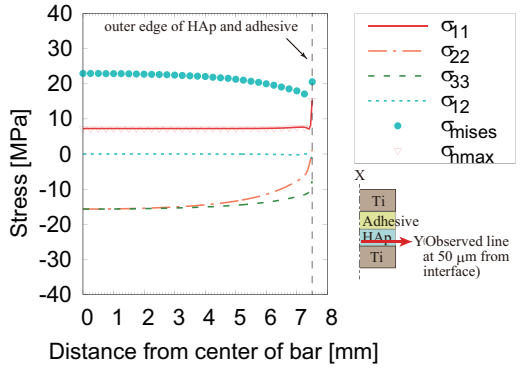

Fig. 11. Stress distribution at a line in HAp coating 50 μm from the interface when it was subjected to maximum loading. Infiltration of adhesive into HAp coating was not considered.

ping. The result quantitatively demonstrates the effectiveness of pre-immersion treatment proposed by Hakozaki et al. [19], which prevents infiltration of the adhesives into HAp coating layer. The values of infiltration ratios of the adhesives were similar regardless of adhesive types, which showed the similar values of interfacial strength.

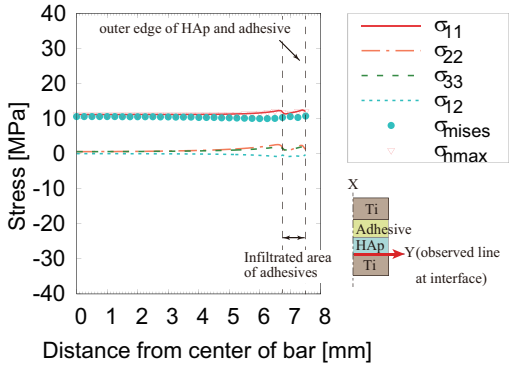

Fig. 12. Stress distribution at the interface between HAp coating and Ti substrate when it was subjected to maximum loading. Infiltration of adhesive into HAp coating was assumed at 10% of HAp coating layer from its outer edge.

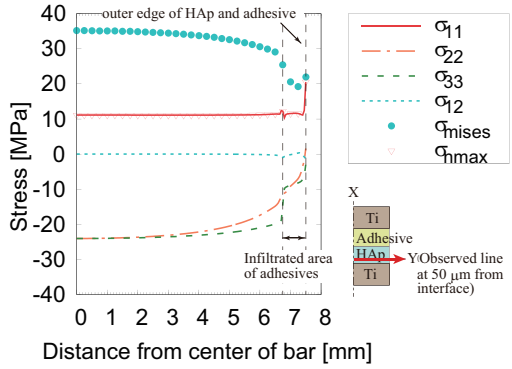

Fig. 13. Stress distribution at a line in HAp coating 50 μm from the interface when it was subjected to maximum loading. Infiltration of adhesive into HAp coating was assumed at 10% of HAp coating layer from its outer edge.

Consequently, prohibiting inflitration of adhesives is a crucial process to determine reliable and rational values of interfacial strength of HAp coating.

Finite element analyses were conducted to systematically discuss the effect of infiltration of adhesives on interfacial strength. **Figs. 10** and **11** show stress distributions in HAp coating or at an interface. In the HAp coating layer, compressive normal stress was developed due to a difference in poisson's ratio between two layers, which increased the value of von mises stress. However, the value of maximum principal stress, which is the determinant factor of interfacial failure, was not affected by the positions. The maximum value of maximum principal stress was always observed at the outer edge of HAp coating. **Figs. 12** and **13** show stress distributions when infiltration of adhesive into HAp coating was assumed at 10% of HAp coating layer from its outer edge. Though the distribution of maximum principal stress was fluctuated by infiltration area of adhesives due to its change in mechanical properties, the position of maximum value in the distribution was unchanged. Therefore, in the cases without considering cohesive failure inside the HAp coating layer,

Table 2. Effect of infiltrating area and infiltration ratio of adhesives into HAp coating on interfacial strength calculated by FEM.

Interfacial strength [MPa]	Infiltration ratio of adhesives 10%	20%	30%	40%	50%
From the center (Case; Center infiltration)	7.83±0.03	7.87±0.02	7.87±0.02	7.91±0.02	7.95±0.02
From the outer edge (Case; Edge infiltration)	13.33±0.04	13.13±0.04	13.12±0.04	13.10±0.04	12.91±0.03
Uniform infiltration	12.42±0.04	12.45±0.04	11.71±0.03	11.72±0.03	13.21±0.03

only the position of infiltration area, not the degree of infiltration, can affect interfacial strength because a value of interfacial strength at infiltrated area was assumed to be the one of adhesives.

Table 2 shows a summary of interfacial strength for various types of infiltration condition. Interfacial strength was calculated by the average maximum principal strength at Ti substrate far from interface layers at maximum loading. In the case of center infiltration (Case; Center infiltration) whose outer edge of HAp coating layer was HAp coating, the values of interfacial strength was not affected by infiltration ratio. The result is rational because failure point was judged by the outer edge of HAp coating. On the contrary in the cases of edge infiltration (Case; Edge infiltration), whose outer edge of HAp coating layer was mixed material of HAp coating with adhesion, its interfacial strength was assumed to be the one of the adhesives and shows higher value regardless of infiltration ratio. In addition, the values of interfacial strength in edge infiltration (Case; Edge infiltration) was slightly decreasing with increasing infiltration ratio. In uniform infiltration case, the values is gradually increasing because mixed layer became more thick at outer edge in higher infiltration ratio. In the experimental result, prevention of infiltration could provide lower possibility of infiltration of adhesives at the outer edge of HAp coating. Therefore, the result in **Table 2** can qualitatively explain the experimental results shown in **Fig. 5** that excessive area of adhesives could enhance interfacial strength of HAp coating. We also observed an effect of young's modulus of adhesives on interfacial strength of HAp coating by the FEA. Without infiltration, Metal Lock Y610 (Young's modulus = 0.7 GPa shown in **Table 1**) provided a slightly higher interfacial strength of 8.83±0.02 MPa than that of 7.83±0.03 MPa by Superbond (Young's modulus = 1.9 GPa shown in **Table 1**). Though mechanical property of adhesives also affects interfacial strength, infiltration feature is the dominant factor in determining the interfacial strength of HAp coating.

Cohesive failure in HAp coating or adhesive layers is also one of considerable factor because fracture surface in **Figs. 6** and **7** shows shearing failure at the outer edge of specimens probably due to cohesive failures. FEM results shown in **Figs. 10** and **11** indicate that cracking can be initiated at the outer edge, which may affect fracture processes of HAp coating layer. Interactions of cohesive/adhesive damages to final fracture are one of considerable factors. Porosity in HAp coating is also changed by infiltrations of adhesive. Such the effects are to be discussed in further study.

The results showed that general adhesives are applicable for interfacial strength testing. We can summarize a way of selecting adhesives as follows;

- Adhesive strength; it should be higher than the one of HAp coating.
- Type of hardening; it should be hardened at ambient temperature with longer periods in order to apply the pre-immersion treatment method to prevent infiltration.
- Color; it should be blighter than the one of substrate in fracture surface observation in order to distinguish the adhesive from substrate or HAp coating with ease.

4. Conclusion

Interfacial strength tests of plasma-sprayed HAp coating were conducted by using general adhesives. The summary of obtained results are the follows;

- Pre-immersion treatment process proposed by Hakozaki et al. [19] could prevent infiltration of adhesives regardless of adhesive types and then reliable results could be obtained by using a general adhesive.
- Determination of infiltration ratio of adhesives by using pictures of fracture surfaces were difficult when the color of adhesives are hardly distinguished from the ones of substrates or HAp coating.
- Raman spectroscopy could quantitatively detect infiltration ratio of adhesives and effectiveness of the pre-immersion treatment process.
- FEM result indicated that prevention of infiltrating at the outer edge of HAp coating layer was effective to detect interfacial strength of HAp coating itself.
- Suitable types of adhesive should possess curable at ambient temperature, longer operative periods/hardening time and higher cohesive strength than the one of interfacial strength between coating with substrates.

Acknowledgements

This study was partly supported by JSPS KAKENHI Grant Number 26870213. We greatly appreciate Niigata Metallicon Co. Ltd. for making plasma-sprayed samples. We are grateful to Dr. Noriyuki Hisamori (Sophia University) and Dr. Mitsuo Niinomi (Tohoku University) for their critical comments on the study.

References:

[1] L. Sun, C. C. Berndt, K. A. Gross, and A. Kucuk, "Material fundamentals and clinical performance of plasma-sprayed hydroxyapatite coatings: A review," J. of Biomedical Materials Research, Vol.58, No.5, pp. 570-592, 2001.
[2] G. Y. Lee, A. Srivastava, D. D. D'Lima, P. A. Pulido, and C. W. Colwell Jr., "Hydroxyapatite-Coated Femoral Stem Survivorship at 10 Years," The J. of Arthroplasty, Vol.20, Supplement 3, pp. 57-62, 2005.
[3] X. Zheng, M. Huang, and C. Ding, "Bond strength of plasma-sprayed hydroxyapatite/Ti composite coatings," Biomaterials, Vol.21, No.8, pp. 841-849, 2000.
[4] H. Guo, K. A. Khor, Y. C. Boey, and X. Miao, "Laminated and functionally graded hydroxyapatite/yttria stabilized tetragonal zirconia composites fabricated by spark plasma sintering," Biomaterials, Vol.24, No.4, pp. 667-675, 2003.
[5] A. Moshaverinia, S. Ansari, M. Moshaverinia, N. Roohpour, J. A. Darr, and I. Rehman, "Effects of incorporation of hydroxyapatite and fluoroapatite nanobioceramics into conventional glass ionomer cements (GIC)," Acta Biomaterialia, Vol.4, No.2, pp. 432-440, 2008.
[6] J. Sakurai and S. Hata, "Characteristics of Ti-Ni-Zr Thin Film Metallic Glasses / Thin Film Shape Memory Alloys for Micro Actuators with Three-Dimensional Structures," Int. J. of Automation Technol., Vol.9, No.6, pp. 662-667, 2015.
[7] J. M. Fernández-Pradas, M. V. García-Cuenca, L. Clèries, G. Sardin, and J. L. Morenza, "Influence of the interface layer on the adhesion of pulsed laser deposited hydroxyapatite coatings on titanium alloy," Applied Surface Science, Vol.195, No.1-4, pp. 31-37, 2002.
[8] T. Matsuya, Y. Otsuka, M. Tagaya, S. Motozuka, K. Ohnuma, and Y. Mutoh, "Formation of stacked luminescent complex of 8-hydroxyquinoline molecules on hydroxyapatite coating by using cold isostatic pressing," Materials Science and Engineering C, Vol.58, pp. 127-132, 2016.
[9] K. Gross, W. Walsh, and E. Swarts, "Analysis of retrieved hydroxyapatite-coated hip prostheses," J. of Thermal Spray Technology, Vol.13, No.2, pp. 190-199, 2004.
[10] T. Laonapakul, Y. Otsuka, A. Nimkerdphol, and Y. Mutoh, "Acoustic emission and fatigue damage induced in plasma-sprayed hydroxyapatite coating layers," J. of the Mechanical Behavior of Biomedical Materials, Vol.8, pp. 123-133, 2012.
[11] T. Laonapakul, A. R. Nimkerdphol, Y. Otsuka, and Y. Mutoh, "Failure behavior of plasma-sprayed HAp coating on commercially pure titanium substrate in simulated body fluid (SBF) under bending load," J. of the Mechanical Behavior of Biomedical Materials, Vol.15, pp. 153-166, 2012.
[12] A. R. Nimkerdphol, Y. Otsuka, and Y. Mutoh, "Effect of dissolution/precipitation on the residual stress redistribution of plasma-sprayed hydroxyapatite coating on titanium substrate in simulated body fluid (SBF)," J. of the Mechanical Behavior of Biomedical Materials, Vol.36, pp. 98-108, 2014.
[13] Y. Otsuka, Y. Miyashita, and Y. Mutoh, "Effects of delamination on fretting wear behaviors of plasma-sprayed hydroxyapatite coating," Mechanical Engineering J., Vol.3, No.2, Paper No.: 15-00573, 2016.
[14] Y. Otsuka, H. Kawaguchi, and Y. Mutoh, "Cyclic delamination behavior of plasma-sprayed hydroxyapatite coating on Ti-6Al-4V substrates in simulated body fluid," Materials Science and Engineering: C, Vol.67, pp. 533-541, 2016.
[15] Y. Otsuka, D. Kojima, and Y. Mutoh, "Prediction of cyclic delamination lives of plasma-sprayed hydroxyapatite coating on Ti-6Al-4V substrates with considering wear and dissolutions," J. of the Mechanical Behavior of Biomedical Materials, Vol.64, pp. 113-124, 2016.
[16] ISO13779-4:2002, "Implants for surgery – Hydroxyapatite – Part 4; Determination of coating adhesion strength," Int. Organization for Standardization, 2002.
[17] ASTMF1147-05, "Standard test for tensile test of calcium phosphate and metallic coatings," ASTM International, 2005.
[18] S. S. Scherrer, P. F. Cesar, and M. V. Swain, "Direct comparison of the bond strength results of the different test methods: A critical literature review," Dental Materials, Vol.26, No.2, pp. e78-e93, 2010.
[19] Y. Hakozaki, Y. Otsuka, Y. Miyashita, and Y. Mutoh, "Effects of adhesives on validity of interfacial strength of plasma-sprayed hydroxyapatite coating," The 10th Asia-Pacific Conf. on Fracture and Strength (APCFS2016), 2016.
[20] O. Shiho, G. K. Y. Koichiro, F. Yuji, K. Wataru, O. Naoki, and M. Hiroyuki, "Mechanical properties of newly developed PMMA resin cement," Adhesive Density, Vol.26, No.1, pp. 8-16, 2008.
[21] R. B. Heimann, "Thermal spraying of biomaterials," Surface and Coatings Technology, Vol.201, No.5, pp. 2012-2019, 2006.

Name:
Yuichi Otsuka

Affiliation:
Department of System Safety, Nagaoka University of Technology

Address:
1603-1 Kamitomioka, Nagaoka, Niigata 940-2188, Japan

Brief Biographical History:
2007 Ph.D. in Engineering, Kyusyu University
2007- Specially-Apointed Associate Professor, Nagaoka University of Technology
2012- Associate Professor, Department of System Safety, Nagaoka University of Technology

Main Works:
• Y. Otsuka, D. Kojima, and Y. Mutoh, "Prediction of cyclic delamination lives of plasma-sprayed hydroxyapatite coating on Ti-6Al-4V substrates with considering wear and dissolutions," J. of the Mechanical Behavior of Biomedical Materials, Vol.64, pp. 113-124, 2016.

Membership in Academic Societies:
• Japan Society of Mechanical Engineers (JSME)
• Japan Society of Material Science (JSMS)
• Japan Society of Biomaterials (JSB)

Name:
Yoshihisa Hiraki

Affiliation:
Nagaoka University of Technology

Address:
1603-1 Kamitomioka, Nagaoka, Niigata 940-2188, Japan

Brief Biographical History:
2017 B.S. in Engineering, Nagaoka University of Technology
2017- Graduate Student, Nagaoka University of Technology

Membership in Academic Societies:
• Japan Society of Mechanical Engineers (JSME)

Name:
Yuki Hakozaki

Affiliation:
Nagaoka University of Technology

Address:
1603-1 Kamitomioka, Nagaoka, Niigata 940-2188, Japan

Brief Biographical History:
2016 B.S. in Engineering, Nagaoka University of Technology
2016- Graduate Student, Nagaoka University of Technology

Membership in Academic Societies:
• Japan Society of Mechanical Engineers (JSME)
• Japan Society of Material Science (JSMS)

Name:
Yukio Miyashita

Affiliation:
Department of Mechanical Engineering, Nagaoka University of Technology

Address:
1603-1 Kamitomioka, Nagaoka, Niigata 940-2188, Japan

Brief Biographical History:
1998 Ph.D. in Engineering, Nagaoka University of Technology
1998- Assistant Professor, Nagaoka University of Technology
2007- Associate Professor, Nagaoka University of Technology

Main Works:
• Y. Farazila, Y. Miyashita, H. Wang, Y. Mutoh, and Y. Otsuka, "Yag laser spot welding of pet and metallic materials," J. of Laser Micro/Nanoengineering, Vol.6, No.1, pp. 69-74, 2011.

Membership in Academic Societies:
• Japan Society of Mechanical Engineers (JSME)
• Japan Society of Material Science (JSMS)
• Japan Welding Engineering Society (JWES)

Name:
Yoshiharu Mutoh

Affiliation:
Nagaoka University of Technology

Address:
1603-1 Kamitomioka, Nagaoka, Niigata 940-2188, Japan

Brief Biographical History:
1979 Ph.D. in Engineering, Osaka University
2012- Vice President, Nagaoka University of Technology
2016- Professor Emeritus, Nagaoka University of Technology

Main Works:
• Y. Mutoh, D. W. Hoeppner, and S. E. Kinyon, "Fretting Fatigue: Advances in Basic Understanding and Applications," ASTM International, 2003.

Membership in Academic Societies:
• Japan Society of Mechanical Engineers (JSME)
• Japan Society of Material Science (JSMS)
• Japan Welding Engineering Society (JWES)